
2019

JOINT INSTITUTE FOR NUCLEAR RESEARCH



DUBNA



VEKSLER AND BALDIN LABORATORY OF HIGH ENERGY PHYSICS

The activity of the Veksler and Baldin Laboratory of High Energy Physics in 2019 was focused on the implementation and further development of the NICA

complex project (the Nuclotron–NICA, MPD, BM@N and SPD subprojects), and participation in the experiments at world-class accelerator centres.

MOST IMPORTANT RESULTS IN THE DEVELOPMENT OF THE NICA COMPLEX

Nuclotron–NICA Project

Booster and Beam Transfer Channels

The main efforts of the accelerator division in 2019 were targeted to the assembling and commissioning of the Booster synchrotron.

HILac–Booster beam transfer line is one of the key elements that provides ions transfer from the ion sources to accelerators with minimal losses. The mounting of the transfer line was finished in July and commissioned in December 2019.

In 2019, the mounting of the Booster subsystems was completed with the installation of the cryomagnetic system. On 23 December, Booster commissioning was officially started. It includes the following stages:

- tuning of the power supply and test of the energy evacuation system;
- test of the vacuum system;
- test of the thermometry and cooling of the cryomagnetic system;

and has to be finished by the end of May 2020. The next stage — test with the ion beam — will start in June 2020.

The civil works on the Booster–Nuclotron transfer line were completed in 2019. Installation, mounting and commissioning of the Booster–Nuclotron transfer line elements are scheduled for 2020.

Collider Ring

The plans on the assembly of the Nuclotron–Collider transfer line and collider ring are strongly correlated with the civil works flow. The status of the collider complex construction by the end of 2019 is as follows:

- piles 100% readiness;
- reinforced concrete structures > 90% readiness;
- metal structure installation > 75% readiness;
- facades installation 10% readiness;
- roofs 30% readiness;
- earth works and temporary roads 90% readiness.

The common delay in the construction is about a year. The main reason is accepted changes in the project after start of the construction, which brings the increase in the building area from 20 to 30 thousand squared meters. It leads to the expansion of the piles field, reinforced concrete and metal structures, roofing and walling areas as well as corresponding increase of engineering equipment — ventilation, refrigeration and power supply systems.

It is expected to start mounting of the collider dipole magnets in the 1st collider arc section, the assembly of the Nuclotron–Collider transfer line and the mounting of the first RF stations in the 3rd quarter of 2020 (see Table 1).

Manufacturing and testing of the collider subsystems equipment were continued in 2019. Almost 35% of the dipoles and 10% of the quadrupoles were assembled and underwent certification on the test bench.

Table 1. Nuclotron–Collider transfer line equipment status

Subsystem	Readiness	Delivery to JINR
Magnets	95%	March 2020
Vacuum chambers and diagnostics	70%	June 2020
Power supplies	10%	August 2020

Detailed information on the collider construction status is available in the 2019 annual review report at http://nucloweb.jinr.ru/nica/MAC/20Jan16_Rpt_to_MAC.pdf.

Cryogenic Complex

The NICA complex includes three SC accelerators and for its operation the power of the existing cryogenic complex has to be significantly extended from 4 to 10 kW of refrigerating capacity at 4.5 K. One of the key elements of the cryogenic complex is the new compressor station which has to be installed in a new building constructed for this purpose. In contrast to the experts' opinion, it was decided to engage the Stroytehninvest company, which has no experience in industrial construction as the main contractor. It leads to the delay in the construction from February 2020 to September 2020.

An upgrade of the cryogenic complex in other directions is going on according to the schedule, and the following equipment has been delivered and installed:

- 1000 m³ helium gasholder;
- 40 m³ liquid helium tank;
- 1000 l/h helium liquefier;
- 2 kW satellite refrigerator;
- 1300 kg/h nitrogen liquefier;
- 500 kg/h nitrogen recondenser;
- two 6600 Nm³/h helium screw compressors;
- three 10740 Nm³/h nitrogen turbo compressors;
- five 20 Nm³ nitrogen receivers.

Computing Infrastructure

The computer offline cluster of the Veksler and Baldin Laboratory of High Energy Physics is one of the four basic components of the distributed computer information infrastructure of the NICA project. The cluster is based on a modular principle and consists of computer and communication equipment, cooling, power supply and fire suppression systems.

In October 2019, the cluster was put into operation in the following configuration: 3500 cores and two disk arrays of 3.5 PB each. In the nearest future, it will be expanded to 5000 CPU cores and 2 × 5 PB disk arrays.

The cluster has an internal 100 Gb/s Ethernet network, connected to the cluster network at 200 Gb/s and to the laboratory network at 100 Gb/s.

User Infrastructure

In 2019, the NICA innovation centre design proposed by the general contractor Arena company was approved. The deadline for the documentation preparation is September 2020.

MPD Experiment

SC Magnet

All civil works in the MPD building have to be completed in the 1st quarter of 2020, after that the process of the MPD magnet installation starts.

The MPD magnet yoke has already been delivered in Dubna, the magnet cryostat with SC coil is ready for cold tests.

Time Projection Chamber

The Time Projection Chamber (TPC) is the main tracking detector of the MPD experiment. The production and tests of structural elements and equipment for installation of the TPC inside the MPD were completed. In 2019, ten out of 24 readout chambers (ROCs) were produced, the verification tests of the readout electronics were started. Status of the TPC readout electronics is presented in Table 2.

Time-of-Flight System

By the end of 2019, the purchase of all detector materials was completed, 25% of all mRPCs were assembled, and the rest will be ready until October 2020. The assembled time-of-flight sectors are passing tests on cosmic rays.

FHCal

The MPD forward detector consists of two arms located at 3.2 m from the interaction point. Each arm consists of 45 individual modules. All modules were produced and now are under tests on the cosmic rays. The production of the Front-End Electronics was completed at the end of 2019. The designing of the support platform for FHCal is close to completion.

ECal

The production of the MPD electromagnetic calorimeter modules was started at two sites in Russia. Start of the production in China is expected soon. First ECal modules will be produced in the 3rd quarter of 2020.

Table 2. Schedule of the work on the TPC readout electronics

Subsystem	Completion date
Testing FEC v1.0	February 2019
SAMPA V4 chips received at Dubna 4500 (all)	June 2019
32 preproduced FE cards (version 2.1) assembled (1/2ROC)	July 2019
Testing of half ROCs equipped with FE cards	August–December 2019
Production of FE cards for 1 ROC and its testing	December 2019 – April 2020
Instrumentation and test of ROCs 2, 3, 4	May 2020
Production of FE cards for 5–14 ROCs (total 14)	July 2020
Production of FE cards for the rest 10 ROCs (total 24)	August 2020

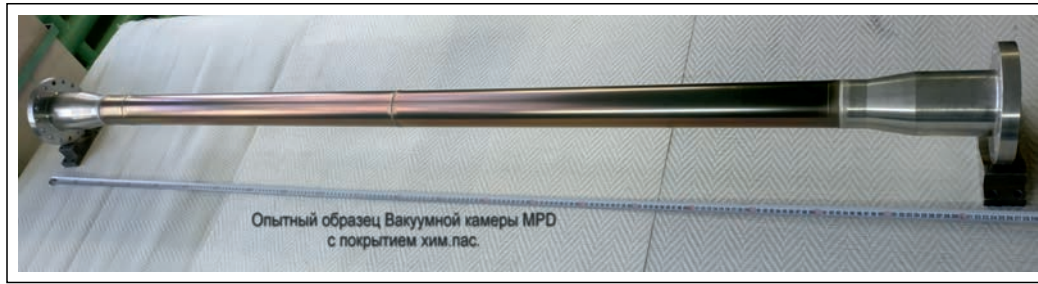


Fig. 1. Prototype of the MPD beam pipe

Beam Pipe

The MPD beam pipe will consist of three parts: central, made of beryllium, and two end parts made of aluminum alloy (Fig. 1).

The production contract for two beryllium beam pipes with the inner diameter of 62 mm was signed in 2019. The production contract for the aluminum parts of the beam pipe is under preparation.

Milestones of the MPD Assembling

Milestones of the MPD assembling are described in Table 3.

MC Simulation and Data Analysis

Five MPD Physics Working Groups (PWG) are created, which cover all MPD physics cases:

- global observables;
- spectra and yields of light flavor hadrons and hypernuclei;
- flow, correlations and fluctuations;
- electromagnetic probes;
- heavy flavor.

In 2019, several reports on the MPD construction status and feasibility study results were given, including those at the international conferences “Quark Matter 2019” and “Strangeness in Quark Matter 2019”.

BM@N Experiment

Data Analysis

The BM@N (Baryonic Matter at the Nuclotron) is the first experiment carried out at the Nuclotron accelerator of the NICA complex. The BM@N scientific programme comprises studies of dense nuclear matter

in heavy-ion beams of the intermediate energy range between the energies of the SIS-18 and NICA/FAIR facilities. The first experimental run was performed in the carbon beam interaction with different nuclear fixed targets.

In 2019, the physics analysis of the obtained experimental data on Λ -hyperon production was performed for interactions of the carbon beam with kinetic energies of 3.5, 4 and 4.5A GeV on C, Al, Cu and Pb nuclei. Results on the cross sections and yields of Λ hyperons were obtained and compared with the predictions of the DCM-QGSM and UrQMD models (Fig. 2).

Spectrometer Status

In 2019, the BM@N team continued the spectrometer preparation for the heavy-ion runs, permanently expanding detectors subsystems:

- Hybrid central tracker based on 7 GEM detectors with the size of the sensitive area of 163×39 cm, which were assembled and tested in collaboration with CERN, and three stations of forward silicon microstrip detectors will operate at the expected rate \sim few 10^5 . The readout electronics of the tracker partially based on IDEAS chips (Norway) was developed.

- For the operation at the rate \sim few 10^6 , expected in 2022, four wide-aperture STS microstrip silicon detector planes were developed in cooperation with the CBM collaboration. The TDR was approved in December 2019.

Table 3. Schedule of MPD assembling

Stage of assembly	Date
MPD hall and pit are ready to store and unpack yoke parts	April 2020
Magnet yoke assembly for the alignment test	May–June 2020
Solenoid is ready for transportation from ASG (Italy)	June 2020
Solenoid delivery in Dubna	July 2020
Assembly of magnet yoke and solenoid	August 2020
Preparation for switching on the solenoid (cryogenics, power supply, etc.)	September 2020
Magnetic field measurement	November 2020
Installation of support frame	December 2020
Installation of the detector subsystems, electronics platform, cabling	January–April 2021
Commissioning	May 2021
Readiness for the cosmic ray tests	June 2021

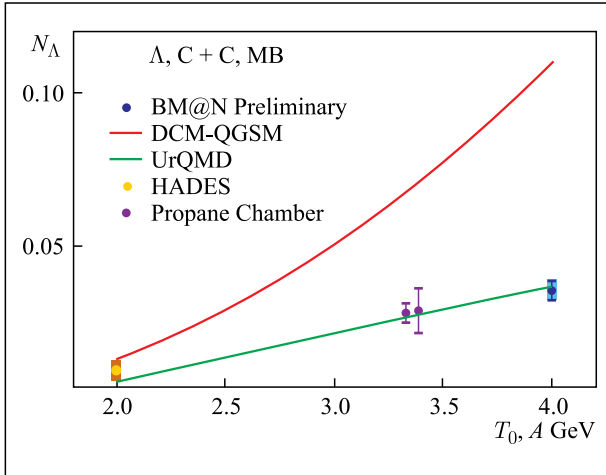


Fig. 2. Yields of Λ hyperons in the BM@N experiment in comparison with models of other experiments

- The outer tracker includes three cathode strip chambers (CSCs) of 113×107 cm for recording tracks for the near time-of-flight system (manufactured) and two large CSCs of 219×145 cm for the far time-of-flight system (designed).

PARTICIPATION IN EXPERIMENTS AT EXTERNAL ACCELERATORS

Experiments at the Large Hadron Collider *ALICE*

During 2019, the femtoscopic correlation analysis of identical charged kaons was finished for p -Pb collisions at 5.02 TeV (per pair of nucleons). The radii of the emission source found during the fit versus pair transverse momentum and the event centrality are shown in Fig. 3 together with the same data obtained before. One can see a good agreement between both types of the kaon pairs.

Such a type of the correlations was studied for the first time in proton-nucleus collisions. The comparison of the radii of the emission source with the ones obtained before for pp and Pb-Pb collisions showed that the radii of the source in p -Pb collisions are closer to those created in pp collisions than in Pb-Pb ones. These phenomena can be an indication of weakness/absence of collective effects in emitting sources in p -Pb interactions and disfavor models with large initial size or strong collective expansion at low multiplicities [1].

The analysis of coherent J/ψ and ρ^0 production in Pb-Pb ultra-peripheral collisions at an energy of 5.02 TeV (per pair of nucleons) was finished in 2019. The differential cross sections were determined and compared with different theoretical model predictions (Fig. 4). The main result is as follows: the best agree-

- A hadron calorimeter (FHCAL) based on MPD and CBM modules to be used in high-intensity heavy-ion beams was manufactured and installed.

The vacuum beam pipe in upstream direction from the target was manufactured and installed. The target station operating with several targets in vacuum was developed.

SPD Experiment

In the framework of the SPD project, the following important results were obtained in 2019.

The first version of SPD CDR was presented at a meeting of the PAC for Particle Physics. Several versions of the SPD magnetic system were considered: hybrid (toroid in the centre + 2 Helmholtz coils in each end face), 6 Helmholtz coils with different configurations of current switching and solenoid.

The first version of tracking in SPD based on the Kalman filter was developed. The momentum resolution for different versions of the magnetic system was obtained. The simulation was carried out to study the Drell-Yan processes, charmonium and direct photons production. The formation of the SPD collaboration was started; a Commission for the preparation of the SPD Constitution was established.

ment with the models was shown in the assumption of moderate effect of gluon shadowing. Besides, the first measurements of the coherent photo-production of ρ meson and resonance-like object with the mass near $1700 \text{ MeV}/c^2$ were performed [2].

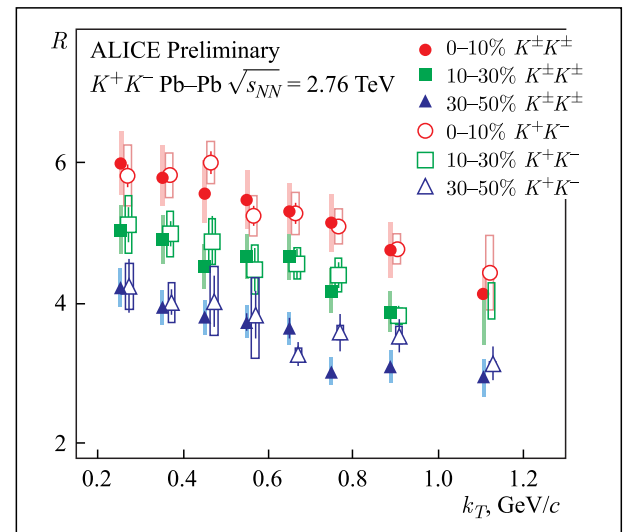


Fig. 3. Radii of the emission source of K^+K^- and identical kaon pairs versus pair transverse momentum and event centrality

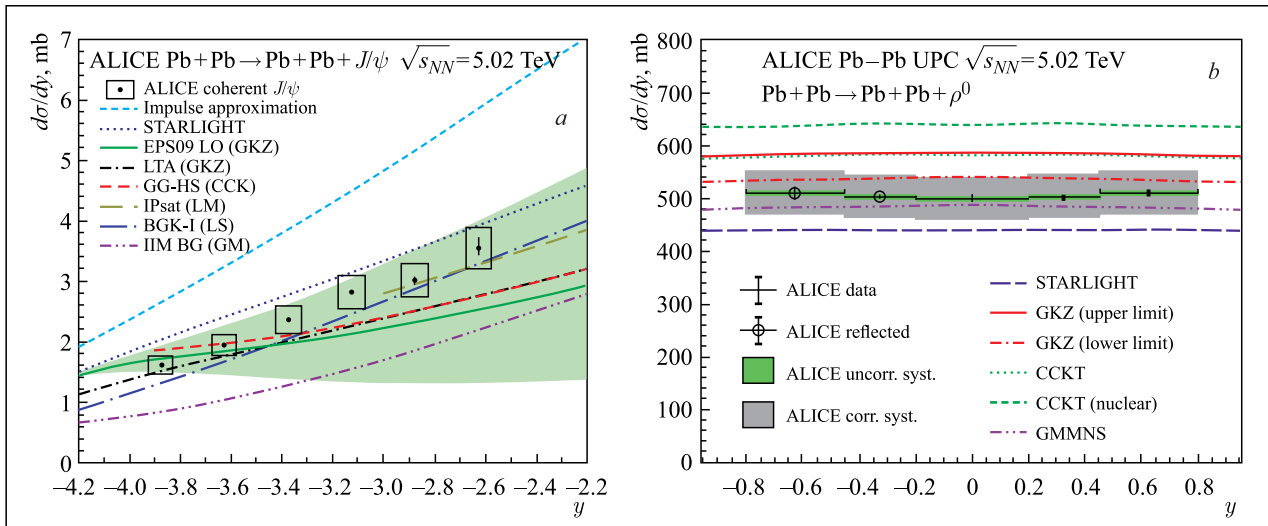


Fig. 4. *a*) Comparison of differential cross sections of the coherent J/ψ production with predictions of various models. *b*) Comparison of differential cross sections of the coherent ρ^0 production with predictions of various models

ATLAS

In 2019, the ATLAS group members were engaged in the following activities: experimental data analysis, simulation of a new process including SUSY particles, participation in the ATLAS detector upgrade programme for high-luminosity environment at HL-LHC as well as QCD analysis of the DIS data.

Cross sections of associated production of a Higgs boson decaying into b -quark pairs and an electroweak gauge boson, W or Z , decaying into leptons were measured as a function of the gauge boson transverse momentum. The measurements were performed in kinematic fiducial volumes defined in the “simplified template cross-section” framework. The results were obtained using 79.8 fb^{-1} of proton–proton collisions recorded by the ATLAS detector at the LHC at a centre-of-mass energy of 13 TeV. All measurements were found to be in agreement with the Standard Model predictions, and limits were set on the parameters of an effective Lagrangian sensitive to modifications of the Higgs boson couplings to the electroweak gauge bosons (Fig. 5).

Participation in the ATLAS detector upgrade programme included irradiation of the optical fibres at the IBR-2 reactor to check radiation hardness of the materials for the applications in the ATLAS detector operating at the HL-LHC. A radiation-resistant analogue signal pre-shaper for the ATLAS endcap hadron calorimeter was designed, and a special setup was developed to measure characteristics of prototypes and then integrated circuits and their certification. The electrical characteristics were measured at this stand, and an agreement was found with the expected ones. The developed circuit of the pre-shaper was used to design the prototype of a solid-state chip. Once the chip is manufactured, its characteristics will also be studied at this stand.

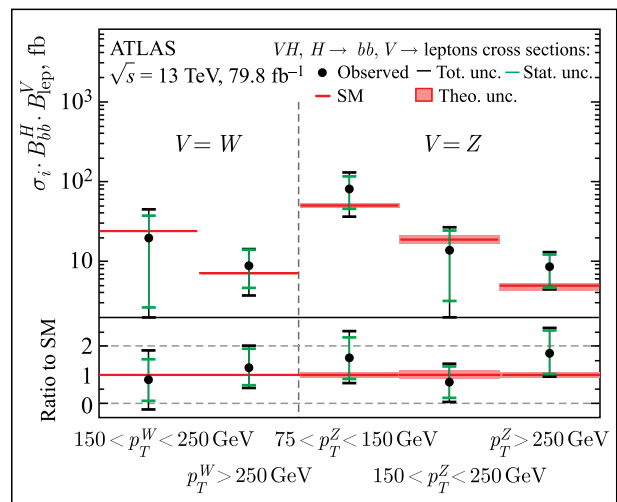


Fig. 5. Measured VH , $V \rightarrow$ leptons simplified template cross sections times the $H \rightarrow \bar{b}b$ branching ratio

CMS

In 2019, the JINR group took part in data processing and physics analysis of data collected during the LHC Run 2 (2015–2018) with the proton beams at an energy of 13 TeV and a luminosity up to $2.14 \cdot 10^{34} \text{ cm}^{-2} \cdot \text{s}^{-1}$.

A search was performed for a narrow resonance decaying to a pair of muons (Fig. 6, *a*) [3]. No significant deviation from the Standard Model (SM) predictions was observed. The 95% CL upper limits were set on the production cross section of this process (Fig. 6, *b*) [3].

The measurements of the differential cross section for the Drell–Yan process, based on proton–proton collision data at a centre-of-mass energy of 13 TeV, collected by the CMS experiment, are in good agreement with the previous ones at $\sqrt{s} = 8 \text{ TeV}$ and consistent with studies of angular characteristics of muons produced in this process [4, 5].

During the CMS Phase-1 Upgrade, the front-end electronics of Hadron Barrel (HB) calorimeter were re-

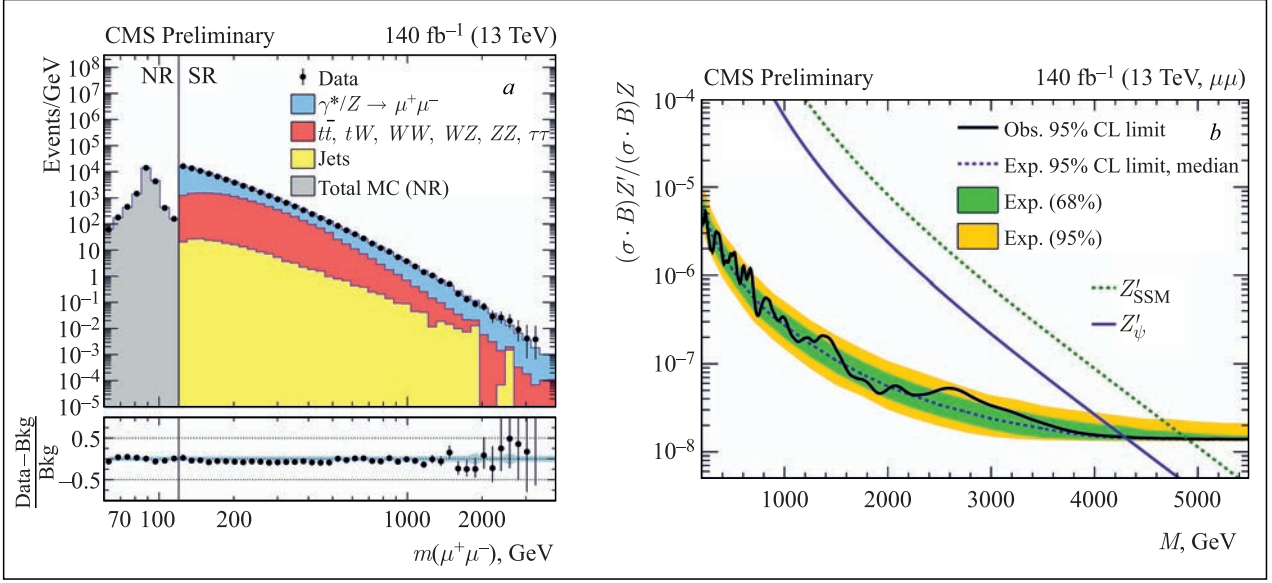


Fig. 6. *a*) The invariant mass distribution of pairs of muons observed at $\sqrt{s} = 13$ TeV in data (black dots with statistical error bars) and expected from the SM processes (stacked histograms) [3]. *b*) The upper limits at 95% CL on the product of production cross section and branching fraction for a spin-1 resonance, relative to the product of production cross section and branching fraction of a Z boson, for the dimuon channel [3]. The shaded bands correspond to the 68% and 95% quantiles for the expected limits. Theoretical predictions for the spin-1 Z'_{SSM} and Z'_{ψ} resonances are shown for comparison

placed with new ones. The JINR group established a test-stand for long-term burn-in tests of readout electronics components using SiPMs for the HB calorimeter. The test-stand infrastructure was fully prepared, namely, the water-cooling system of the readout modules, low-voltage power supply system, SiPMs bias voltage supply system, fiber optic communication system of the readout electronics, as well the crates with the data-acquisition and trigger systems, control and data recording.

In the framework of the CMS Phase-2 Upgrade, the JINR physicists participated in the Cathode Strip Chambers (CSC) electronics upgrade in four muon stations ME1/1, ME2/1, ME3/1 and ME4/1. A total of 180 chambers were replaced from CMS, moved to the surface laboratory, refurbished with the new electronics, tested and finally reinstalled in the experimental cavern. For ME1/1 chambers, 72 new cooling circuits were manufactured.

Experiments at the CERN Super Proton Synchrotron

COMPASS

In 2019, COMPASS continued the analysis of data collected in 2002–2018.

COMPASS performed the most comprehensive resonance-model fit of $\pi^-\pi^-\pi^+$ states using the results of previously published partial-wave analysis (PWA) of a large data set of diffractive-dissociation events from the reaction $\pi^- + p \rightarrow \pi^-\pi^-\pi^+ + p$ recoil with a 190 GeV/c pion beam [6]. The PWA results are subjected to a resonance-model fit using Breit–Wigner

amplitudes to simultaneously describe a subset of 14 selected waves using 11 isovector light-meson states. For the first time, the t' dependence of the phases of the production amplitudes was determined and it was confirmed that the production mechanism of Pomeron exchange is common to all resonances.

The transverse spin asymmetries measured in semi-inclusive lepto-production of hadrons, when weighted with the hadron transverse momentum P_T , allow for the extraction of important transverse-momentum-dependent distribution functions [7]. The results are compared to the standard unweighted Sivvers asymmetries and used to extract the first transverse moments of the Sivvers distributions for u and d quarks.

COMPASS published the results on the measurement of hard exclusive π^0 muo-production on the proton using 160 GeV/c polarized μ^+ and μ^- beams of the CERN SPS impinging on a liquid hydrogen target. From the average of the measured μ^+ and μ^- cross sections, the virtual-photon proton cross section is determined as a function of the squared four-momentum transfer between initial and final protons in the range $0.08 (\text{GeV}/c)^2 < |t| < 0.64 (\text{GeV}/c)^2$. These results provide important input for modelling the Generalized Parton Distributions (GPD). In the context of the phenomenological Goloskokov–Kroll model, the statistically significant transverse–transverse interference contribution constitutes clear experimental evidence for the chiral-odd GPD \bar{E}_T .

NA61/SHINE

In 2019, the activity of the NA61/SHINE collaboration was aimed at the detector upgrade programme for

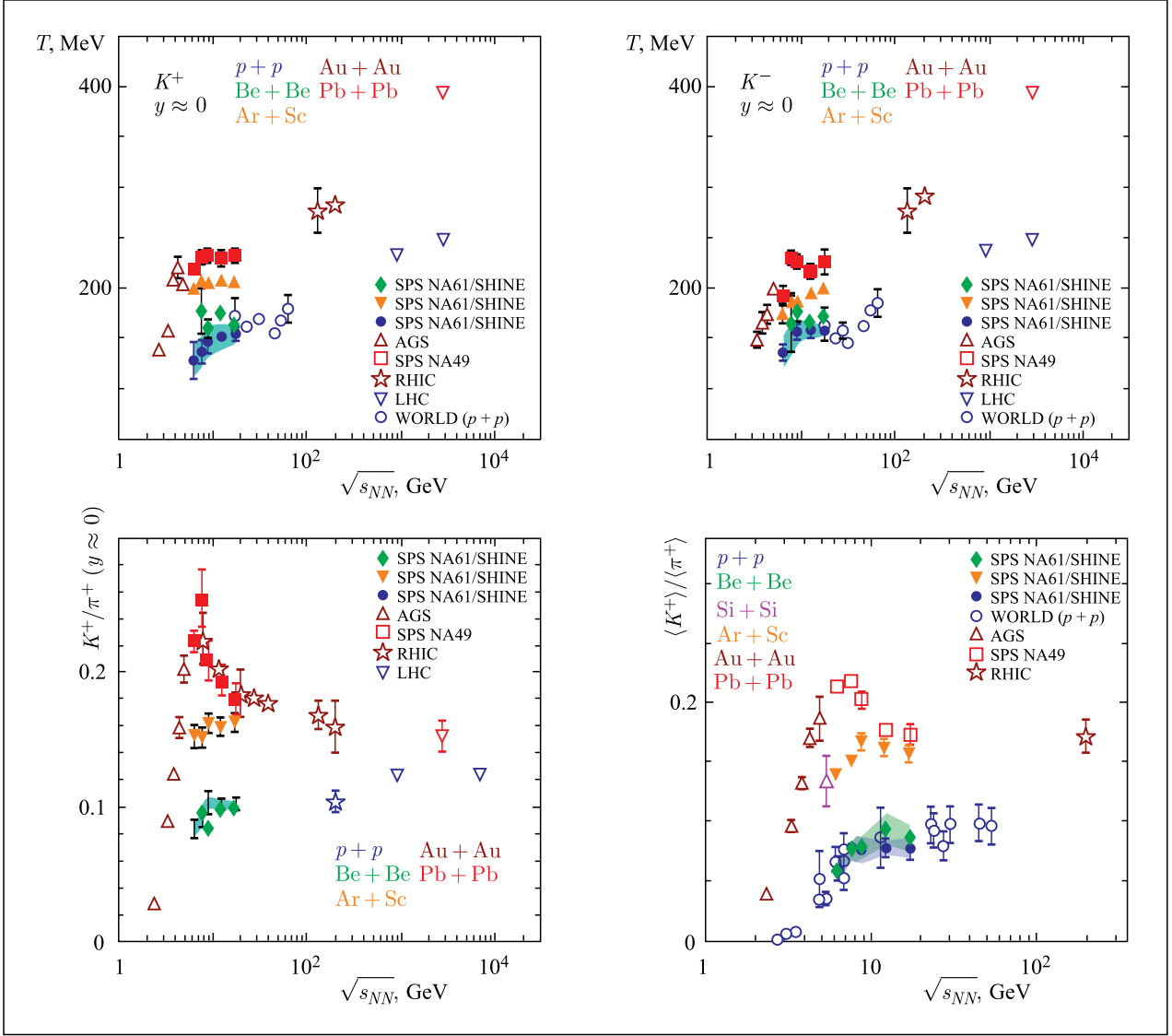


Fig. 7. Inverse slope parameter of mid-rapidity transverse mass spectra of K^+ and K^- mesons as a function of collision energy for $p + p$, Be + Be, Ar + Sc and Pb + Pb/Au + Au collisions (top). K^+/π^+ ratio at mid-rapidity and $\langle K^+ \rangle / \langle \pi^+ \rangle$ ratio in full 4π phase space as a function of collision energy for $p + p$, Be + Be, Ar + Sc and Pb + Pb/Au + Au collisions (bottom)

post-LS2 running in parallel to the physics analysis of data collected before 2019.

The most recent results relate to the particle production properties as well as event-by-event fluctuations in $p + p$, Be + Be and Ar + Sc interactions at beam energies of 19/20, 30, 40, 75/80 and 158A GeV.

Figure 7 shows the current status of the well known “step” and “horn” plots. In Pb + Pb collisions such structures were predicted due to mixed phase of hadron gas (HG) and quark–gluon plasma (QGP). A rapid “horn” change was found in energy dependence of K/π in central Pb + Pb and Au + Au, which was interpreted as due to the onset of deconfinement. The NA61 experiment supplemented these data with the new measurements on $p + p$, Be + Be and Ar + Sc reactions, which exhibit unexpected and very interesting features:

- The energy dependence shows plateau similar to the one observed in $p + p$ interactions.

- The results from Be + Be collisions are close to those from $p + p$ interactions.

- The new data on Ar + Sc interactions show dependence on collision energy qualitatively similar to the $p + p$ data, but the plateau is at significantly higher level.

The $p + p$ results obtained by NA61 have been considered as a possible hint of the onset of deconfinement in small systems.

Surprisingly, there is no indication of “horn” structure in the Ar + Sc data.

NA62 (NA48/2)

The analysis of the NA48/2 and NA62 experimental data was continued in 2019.

The first NA62 result on the search for the $K^+ \rightarrow \pi^+ \nu \bar{\nu}$ decay based on a small subsample of the data collected in 2016 (corresponding to $1.21 \cdot 10^{11}$ K^+ decays) was published [8] (Fig. 8). The single event sensitivity

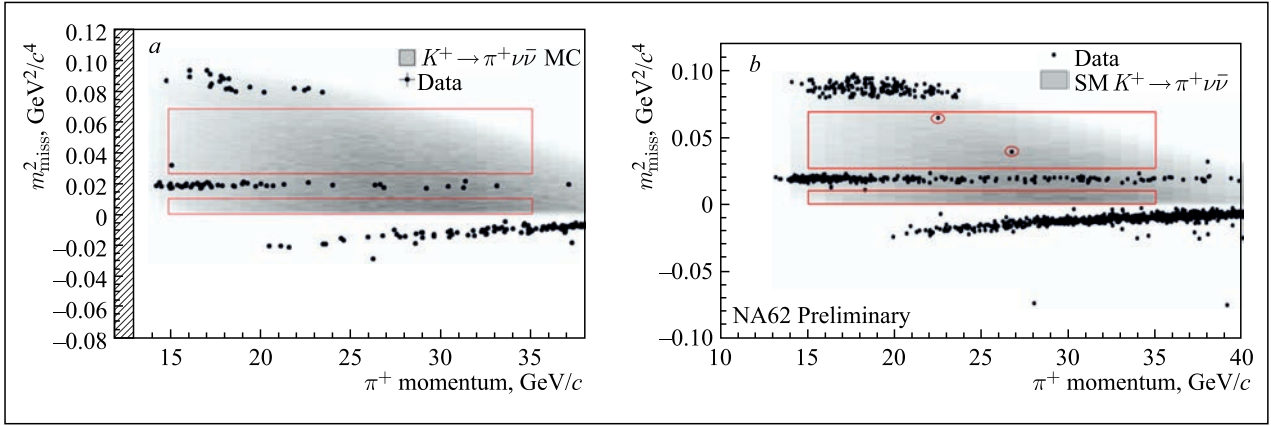


Fig. 8. *a*) One $K^+ \rightarrow \pi^+ \nu \bar{\nu}$ decay candidate revealed in the signal area (red rectangles) as a result of the blind analysis of the data collected by NA62 in 2016; *b*) two $K^+ \rightarrow \pi^+ \nu \bar{\nu}$ decay candidates revealed in the NA62 signal area (red rectangles) after the blind analysis of data collected in 2017

was $3.15 \cdot 10^{-10}$, corresponding to 0.267 of the Standard Model events. One signal candidate was observed while the expected background was 0.152 events. This leads to an upper limit of $14 \cdot 10^{-10}$ on the $K^+ \rightarrow \pi^+ \nu \bar{\nu}$ branching ratio at 95% CL. An analysis of the data collected in 2017 resulted in the selection of two more $K^+ \rightarrow \pi^+ \nu \bar{\nu}$ candidates. With the total expected background of 1.65 ± 0.31 events, the selected three candidates lead to the upper limit of $18.5 \cdot 10^{-10}$ at 90% CL for the $K^+ \rightarrow \pi^+ \nu \bar{\nu}$ branching ratio.

The final article on the results of the NA48/2 analysis of the rare decay $K^\pm \rightarrow \pi^\pm \pi^0 e^+ e^-$ was published [9]. The obtained results are based on $1.7 \cdot 10^{11}$ charged kaon decays recorded in 2003–2004. A sample of 4919 candidates with 4.9% background contamination allows the determination of the branching ratio $BR = (4.24 \pm 0.14) \cdot 10^{-6}$. A study of the kinematic space shows evidence for a structure-dependent contribution in agreement with predictions based on Chiral Perturbation Theory (ChPT). Several P- and CP-violating asymmetries were also evaluated.

The results of the search for the π^0 decays to a photon and an invisible massive dark photon in the NA62 experiment at the CERN SPS were published [10]. From a total of $4.12 \cdot 10^8$ tagged π^0 mesons, no signal was observed. Assuming a kinetic-mixing interaction, limits were set on the dark photon coupling to the ordinary photon as a function of the dark photon mass, improving on previous searches in the mass range 60–110 MeV/c^2 . The results are interpreted in terms of an upper limit of the branching ratio of the electro-weak decay $\pi^0 \rightarrow \gamma \nu \bar{\nu}$, improving the current limit by more than three orders of magnitude.

On the basis of the NA62 experimental data, a new search for the double neutrinoless kaon decays $K^+ \rightarrow \pi^- e^+ e^+$ and $K^+ \rightarrow \pi^- \mu^+ \mu^+$ was performed at the world best level of sensitivity [11]. These decays violate lepton number conservation, and their detection would reveal neutrino Majorana nature that would as-

sume modification of the Standard Model. Expected estimated background in the signal region was found to be 0.16 ± 0.03 and 0.91 ± 0.41 events, while the number of the observed events is 0 and 1, correspondingly. It leads to the upper limits for the branching ratios $2.2 \cdot 10^{10}$ and $4.2 \cdot 10^{11}$ at 90% confidence level, correspondingly. The obtained result improves the world data precision on the eventual lepton number non-conservation. The 2018-year data analysis will further improve the result precision.

NA64

In 2019, the JINR group participated in the analysis of 2016–2018 runs data performed by the collaboration and continued working on the development of a new straw-tube based chambers for the spectrometer upgrade.

In a search for sub-GeV dark matter production mediated by a new vector boson A' , called dark photon in

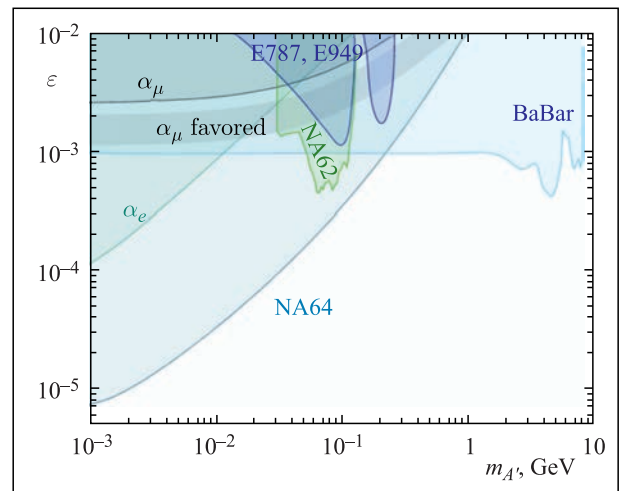


Fig. 9. The NA64 90% CL exclusion region in the $(m_{A'}, \epsilon)$ plane. Constraints from the E787 and E949, BaBar and recent NA62 experiments, as well as the muon α_μ favored area, are also shown

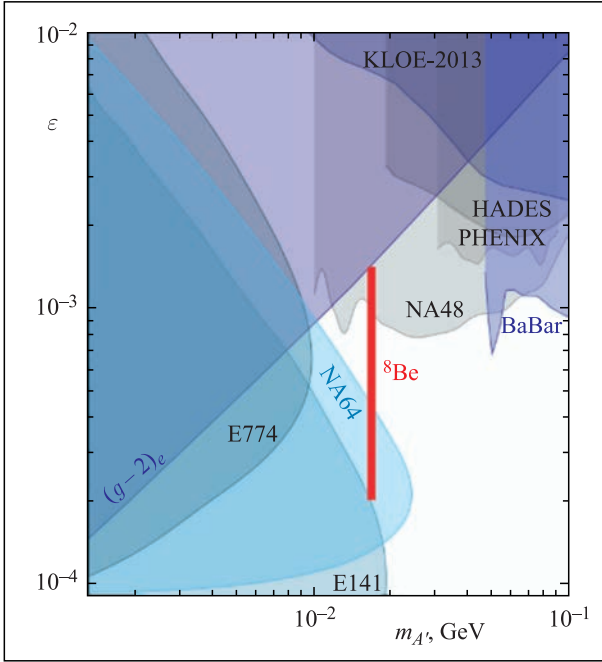


Fig. 10. The 90% CL exclusion areas in the $(m_X; \varepsilon)$ plane from the NA64 experiment (blue area). For a mass of 16.7 MeV, the $X-e^-$ coupling region excluded by NA64 is $1.2 \cdot 10^{-4} < \varepsilon_e < 6.8 \cdot 10^{-4}$. The full allowed range of ε_e explaining the ${}^8\text{Be}^*$ anomaly, $2.0 \cdot 10^{-4} < \varepsilon_e < 1.4 \cdot 10^{-3}$, is also shown (red area). The constraints on the mixing from the experiments E774, E141, BaBar, KLOE, HADES, PHENIX, NA48, and bounds from the electron anomalous magnetic moment $(g-2)_e$ are also shown

missing energy events, from the analysis of the data collected in the years 2016, 2017 and 2018 with $2.84 \cdot 10^{11}$ electrons on target, no evidence of such a process has been found. The results were published in “Physical Review Letters” and highlighted as “the Editor’s suggestion” [12] (Fig. 9).

A combined analysis of the data samples (8.4×10^{10} eot) collected in 2017 and 2018 in the direct search for a new X (16.7 MeV) boson that could explain the anomalous excess of e^+e^- pairs observed in the decays of the excited ${}^8\text{Be}^*$ nucleus (“beryllium anomaly”) was performed. The X boson could be produced in the bremsstrahlung reaction $e^-Z \rightarrow e^-ZX$ by a high-energy beam of electrons incident on the active target and observed through its subsequent decay into e^+e^- pair. No evidence for such decays was found. This allows setting new limits on the $X-e^-$ coupling in the range $1.2 \cdot 10^{-4} < \varepsilon_e < 6.8 \cdot 10^{-4}$, excluding part of the parameter space favored by the beryllium anomaly [13] (Fig. 10).

The NA64 experiment was highlighted by CERN Vice-Director-General E. Elsen in the New Year presentation: “. . . From a wide variety of fixed-target experiments I chose NA62 and NA64 as the most indicative in terms of the potential for discovering new physics at SPS. Analysis of data collected during 2016–2018 with electrons allowed NA64 to achieve a record sensitivity for the region of light dark matter parameters, as well as significantly advance in the search for other new weakly interacting particles.”

EVENTS

1. The 3rd Collaboration Meeting of the MPD and BM@N Experiments at the NICA Facility was held on 16–17 April.

2. International Workshop “SPD at NICA” was held at VBLHEP on 4–8 June.

3. On 11 October, in Mexico, the Collaboration Agreement was signed with:

- National Autonomous University of Mexico,
- Institute for Nuclear Science,
- Meritorious Autonomous University of Puebla,
- Research & Advanced Studies Centre,
- University of Colima,
- Autonomous University of Sinaloa.

4. The 4th MPD Collaboration Meeting of the MPD Experiment was held at Warsaw University of Technology on 22–25 October. Five Polish scientific centres became participants of the MPD collaboration:

- Jan Kochanowski University;
- National Centre for Nuclear Research (NCBJ), Otwock;
- University of Wroclaw;
- Warsaw University of Technology;
- University of Warsaw.

5. The 4th Collaboration Meeting of the BM@N Experiment at the NICA Facility was held on 14–15 October.

REFERENCES

1. Acharya S. et al. (ALICE Collab.). One-Dimensional Charged Kaon Femtoscopy in p -Pb Collisions at $\sqrt{s_{NN}} = 5.02$ TeV // Phys. Rev. C. 2019. V. 100. P. 024002.
2. Acharya S. et al. (ALICE Collab.). Coherent J/ψ Photoproduction at Forward Rapidity in Ultra-peripheral Pb-Pb Collisions at $\sqrt{s_{NN}} = 5.02$ TeV // Phys. Lett. B. 2019. V. 798. P. 134926.

3. *Sirunyan A. M. et al. (CMS Collab.)*. Search for a Narrow Resonance in High-Mass Dilepton Final States in Proton–Proton Collisions Using 140 fb^{-1} of Data at 13 TeV. CMS-PAS-EXO-19-019.
4. *Gorbunov I., Lanev A., Shalaev V., Shmatov S.* Study of Drell–Yan Process with the Compact Muon Solenoid Experiment at the Large Hadron Collider // J. Belarus. State Univ. Phys. 2019. V.2. P. 16–25.
5. *Zygunov V. A.* Final-State Two-Loop Radiative Corrections to the Drell–Yan Process at the LHC in the Soft-Photon Approximation // Phys. Atom. Nucl. 2019. V. 82. P. 183–190.
6. *Aghasyan M. et al. (COMPASS Collab.)*. Light Isovector Resonances in $\pi^- p \rightarrow \pi^- \pi^- \pi^+ p$ at 190 GeV/c // Phys. Rev. D. 2018. V.98. P.092003; CERN-EP/2018-021; hep-ex/1802.05913.
7. *Alexeev M. G. et al. (COMPASS Collab.)*. Measurement of P_T -Weighted Sivers Asymmetries in Lepton-production of Hadrons // Nucl. Phys. B. 2019. V.940. P. 34; CERN-EP/2018-242; hep-ex/1809.02936.
8. *Cortina Gil E. et al. (NA62 Collab.)*. First Search for $K^+ \rightarrow \pi^+ \nu \nu$ Using the Decay-in-Flight Technique // Phys. Lett. B. 2019. V.791. P. 156–166.
9. *Batley J. R. et al. (NA48/2 Collab.)*. First Observation and Study of the $K^\pm \rightarrow \pi^\pm \pi^0 e^+ e^-$ Decay // Phys. Lett. B. 2019. V.788. P. 552–561.
10. *Cortina Gil E. et al. (NA62 Collab.)*. Search for Production of an Invisible Dark Photon in π^0 Decays // JHEP. 2019. V.1905. P. 182.
11. *Cortina Gil E. et al. (NA62 Collab.)*. Searches for Lepton Number Violating K^+ Decays // Phys. Lett. B. 2019. V.797. P. 134794.
12. *Banerjee D. et al. (NA64 Collab.)*. Dark Matter Search in Missing Energy Events with NA64 // Phys. Rev. Lett. 2019. V.123. P. 121801.
13. *Banerjee D. et al. (NA64 Collab.)*. Improved Limits on a Hypothetical $X(16.7)$ Boson and a Dark Photon Decaying into $e^+ e^-$ Pairs. CERN-EP-2019-284; arXiv:1912.11389v1 [hep-ex], 2019.